Int. J. Electrochem. Sci., 12 **(2017)** 3443 – 3458, doi: 10.20964/2017.04.16

International Journal of
ELECTROCHEMICAL
SCIENCE
www.electrochemsci.org

Electrochemical DNA Biosensor Based on Graphene Oxide-Chitosan Hybrid Nanocomposites for Detection of Escherichia Coli O157:H7

Shichao Xu[1,2,3,*], *Yiyi Zhang*[1], *Kai Dong*[1], *Junnan Wen*[1], *Chunming Zheng*[1,2], *Shihuai Zhao*[1,2]

[1] School of Environmental and Chemical Engineering, Tianjin Polytechnic University, 399 Binshui West Road, Tianjin 300387, China
[2] State Key Laboratory of Hollow Fiber Membrane Materials and Membrane Process, Tianjin Polytechnic University, 399 Binshui West Road, Tianjin 300387, China
[3] Tianjin Engineering Center for Safety Evaluation of Water Quality & Safeguards Technology, Tianjin Polytechnic University, 399 Binshui West Road, Tianjin, 300387, China
[*]E-mail: xushichao@tjpu.edu.cn

Received: 12 January 2017 / *Accepted:* 6 February 2017 / *Published:* 12 March 2017

In this article, we present a simple and sensitive electrochemical DNA biosensor based on graphene oxide (GO)/chitosan (CS) hybrid nanocomposites modified glassy carbon electrode (GCE) for detection of Escherichia coli O157:H7 (E.coli O157:H7). The morphology and composition of GO and hybrid nanocomposites were characterized by transmission electron microscope (TEM), X-ray powder diffraction (XRD), field emission scanning electron microscopy (FESEM), and Fourier transform infrared spectrum (FTIR). Cyclic voltammetry investigations indicated that the GO/CS/GCE showed excellent electron transfer ability and good linear relation. Under the optimal hybridization conditions, electrochemical impedance spectroscopy (EIS) responses of ssDNA/GO/CS/GCE biosensor were in linear with the target DNA in the concentration range from 1×10^{-14} to 1×10^{-8} M with the detection limit as 3.584×10^{-15} M (3σ). Moreover, differential pulse voltammetry (DPV) studies revealed good specificity and excellent ability of ssDNA/GO/CS/GCE biosensor to distinguish complementary, 1-base mismatched DNA, 2-base mismatched DNA and multi-base mismatched DNA. The developed strategy in this research revealed that the GO/CS modified electrode possess excellent performance for detecting of Escherichia coli O157:H7 DNA.

Keywords: Graphene oxide, chitosan, nanocomposites, Electrochemical DNA biosensor, Escherichia coli

1. INTRODUCTION

Escherichia coli (E. coli) O157:H7 is one of the most dangerous of the bacterial pathogens that cause serious illnesses including hemorrhagic colitis and hemolytic uremic syndrome, which may lead

to death [1-5]. Most of conventional methods for bacterial detection involve enrichment, isolation and detection steps [6]. These steps tend to be expensive, time consuming, and require highly trained personnel. Therefore, it is desirable to develop a rapid, simple and sensitive analytical method for detection of E. coli to prevent catastrophic outbreaks. Recently, electrochemical DNA biosensor has attracted widespread attention because of its high sensitivity, specificity, low cost, rapidness, simplicity and high accuracy [7, 8]. During fabrication of an electrochemical DNA biosensor, it is critical that immobilize the probe DNA on modified electrode , since it can prominently influence the performances of biosensor [9].

In recent years, a variety of hybrid nanocomposites were synthesized and utilized as substrate materials for DNA immobilization in consequence of their exceptional properties including high surface-to-volume ratios, outstanding biocompatibility, and good electroactivity [10]. Chitosan [β-(1,4)-2-amino-2-deoxy-dglucopyranose] (CS) is the synthetic product of controlled chitin deacetylation [11]. Due to its functional properties, such as biocompatibility [12], biodegradability [13], multiple functional groups, excellent capability of film formation [14, 15] and good water permeability [16], chitosan has attracted great attention in many fields: biotechnology , human [17, 18], pharmacy [19], food engineering [20], environmental technology [21] and biofabrication materials [22]. One of the most important advantages of chitosan is good biocompatibility, it is conducive to form uniform films and determine the integrity and lifetime of the entrapped biomolecules, which is crucial for improving the stability and reproducibility of biosensors. Thus it has been generally used in the immobilization of biomacromolecular on biosensor surface [23]. Xia et al. reported an enzymatic biosensors by controllable chitosan electrodeposition technology [24]. Tiwari et al. developed an electrochemical genosensor based on graphene oxide modified iron oxide–chitosan hybrid nanocomposite for pathogen detection [25]. However, there were few reports about developing the CS-based DNA surface fixation works in the field of E.coli biosensors.

Graphene oxide (GO) with multifarious oxygenated functional groups [26-28], is considered as a precursor for graphene synthesis by thermal reduction processes [29-31]. Owing to its favorable electron mobility and unique surface properties, GO displays excellent property in electrochemistry. Moreover, GO can accommodate active species and promote their electron transfer at the electrode surfaces [32, 33], it is feasible that graphene oxide modified electrode used in electrochemical sensors. Lin's group have reported a sensitive electrochemical biosensor based on a magnetic graphene oxide modified Au electrode to detect vascular endothelial growth factor in human plasma for cancer diagnosis [34]. Reza et al. have investigated a electrochemical based on reduced graphene oxide sheets and chitosan polymer for detection of bisphenol A (BPA) [35].

The GO surfaces negatively charged when dissolved in water, as a result of the ionization of carboxylic acids and hydroxyl groups [36-38]. On the other hand, CS with -NH_2 and -OH in each unit could be protonated to polycationic material in acidic medium, which promoted the interaction between polymer chains and GO sheets [16, 39]. Then, the amino labeled ssDNA probe with both covalent and electrostatic bonding to modified electrode, the former depending on connection between –NH_2 in DNA chains and –COOH on GO surface, the latter depending on attraction between protonated groups in chitosan and anionic phosphate groups in DNA backbone [40, 41]. Thus, GO/CS hybrid nanocomposites modified electrode with good reproducibility and stability is expected.

Hence, in this study, we synthesized GO/CS hybrid nanocomposites in simple steps successfully and coated on glassy carbon electrode (GCE). Further, a DNA biosensor was fabricated by immobilizing probe sequence specific to E. coli. Cyclic voltammetry was used to study the electrochemical behaviors of modified electrode, thereby confirmed the best ratio of GO and CS. Optimum conditions for E. coli measurement and detection limit were investigated by electrochemical impedance spectroscopy (EIS). Electrochemical transduction of the hybridization reaction66 with complementary target DNA, 1-base mismatched DNA, 2-base mismatched DNA and multi-base mismatched DNA have been carried out via differential pulse voltammetry (DPV) response.

2. EXPERIMENTAL

2.1. Reagents and materials

Graphite, chitosan (CS), N-(3-dimethylamminopropyl)-N'-ethylcarbodiimide hydrochloride (EDC), N-hydroxysulfosuccinimid sodium salt (NHS), Tris(hydroxymethyl)-aminomethane, ethylenediaminetetraacetic acid (EDTA) and methylene blue (MB) were all purchased from Shanghai Aladdin Industrial Corporation Co. LTD (Shanghai, China). Acetic acid, sulphuric acid, potassium permanganate, and peroxide were purchased from Tianjin Fengchuan Chemical Reagent Technologies Co. LTD (Tianjin, China). All reagents were of analytical grade and used without further purification.

2.2. DNA sequences

- Probe DNA

5'-NH_2-$(CH_2)_6$-ATG TAC AGC TAA TCC TTG GCC-3'

- Target DNA

5'-GGC CAA GGA TTA GCT GTA CAT-3'

- base mismatched DNA

5'-GGC CAT GGA TTA GCT GTA CAT-3'

- 2-base mismatched DNA

5'-GGC CAT GGA TTA GGT GTA CAT-3'

- multi-base mismatched DNA

5'-ATTGATGGATTAGGTGTACAT-3'

These DNA sequences were synthesized by Shanghai Invitrogen Biotechnology Co. LTD (Shanghai, China).

All stock solutions of the oligonucleotides were prepared with TE buffer solution (10.0 mM Tris-HCl, 1.0 mM EDTA, pH=8.0) and stored at -20 ℃ prior to use. 50 mM Tris-HCl buffer solution containing 20 mM NaCl (pH=7.2) as a washing buffer. The 2×SSC buffer was employed as hybridization solution and prepared containing 0.3 M NaCl and 0.03 M sodium citrate (pH= 7.0). All these solutions were prepared with ultrapure water.

2.3. Apparatus

The cyclic voltammetry (CV), electrochemical impedance spectroscopy (EIS) and differential pulse voltammetry (DPV) were performed using a LK2010 electrochemistry workstation (LANLIKE, China). All experiments were carried out using a three-electrode system consisting of a GO/CS nanocomposite modified GCE (3 mm in diameter, ALS, Japan) as working electrode, a saturated calomel electrode (SCE) as reference electrode and a platinum wire as auxiliary electrode. Transmission electron microscopy (TEM) measurement of the GO was collected from a JEOL-2100. The morphology of the GO/CS nanocomposites was observed via field emission scanning electron microscopy (FESEM, S4800, HITACHI, Japan). The functional groups on the surface of GO and CS were determined by Fourier transform infrared spectrum (Thermo Fisher, Nicolet 6700, USA). X-ray diffraction (XRD) experiments were obtained on DMAX-2500 (Rigaku, Japan).

2.4. Synthesis of GO/CS Nanocomposites

Graphene oxide (GO) was prepared by the modified Hummers method. GO was dissolved in ultrapure water and treated with ultrasound for 1h. At room temperature 0.5 g of CS was added to 2% (v/v) aqueous acetic acid solution (100 mL) and stirred for 2 h. Finally, the GO solution was added into the CS solution and the mixture was further sonicated for 1 h at ambient temperature until a homogeneous dispersion was obtained.

2.5. Fabrication of electrochemical DNA biosensor

The 3 mm diameter glassy carbon electrode was polished with 0.3 μm and 0.05 μm alumina slurry, followed by sonication in 0.5 M HNO_3, ethanol and ultrapure water for 30 s, respectively, and finally dried with nitrogen. Next, 10 μL of the prepared GO/CS suspension solution was dripped onto the clean GCE and dried at an ambient temperature for 24 h to form the modified electrode, which was named as GO/CS/GCE. Afterward, the GO/CS/GCE was placed in 5 μL amino-labeled probe DNA solution and 10 μL Tris-HCl buffer (containing 25 mM EDC and 10 mM NHS) at 40℃ for 1 h. The electrode was then rinsed with washing solution to remove unbound DNA and stored at 4℃ until use. The biosensor obtained was denoted as ssDNA/GO/CS/GCE.

2.6. Hybridization procedure and electrochemical detection

Hybridization reaction was carried out by immersing the ssDNA/GO/CS/GCE into 2×SSC buffer solution with the different concentrations of complementary target DNA for 50 min at 25℃. Then the obtained electrode was rinsed with washing solution to remove the extra ssDNA. This electrode was further named as dsDNA/GO/CS/GCE. The dsDNA/GO/CS/GCE was immersed into Tris-HCl buffer (pH=7.2) containing 10 μM MB and 20 mM NaCl for 5 min with stirring to accumulate the electrochemical indicator and utilized for electrochemical detection of E. coli. The

fabrication and detection process of the biosensor was representing in Scheme 1. The chemistry of prepared biosensor was shown in Scheme 2.

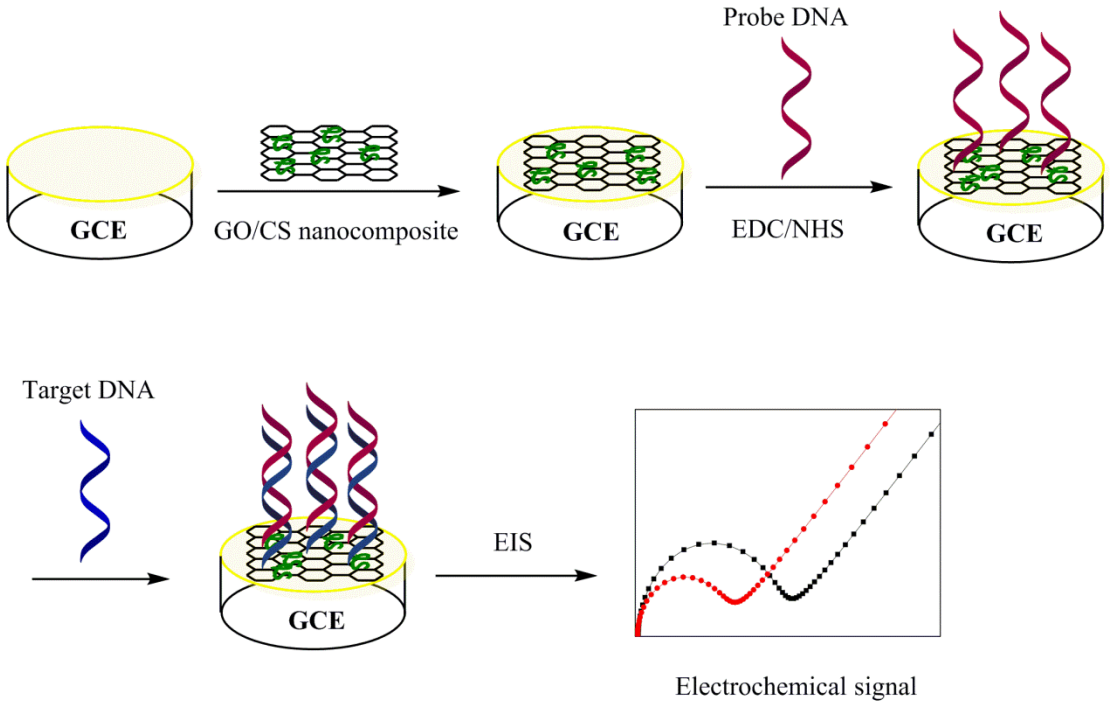

Scheme 1. Schematic illustration of the fabrication of electrochemical DNA biosensor for detection of Escherichia coli O157:H7.

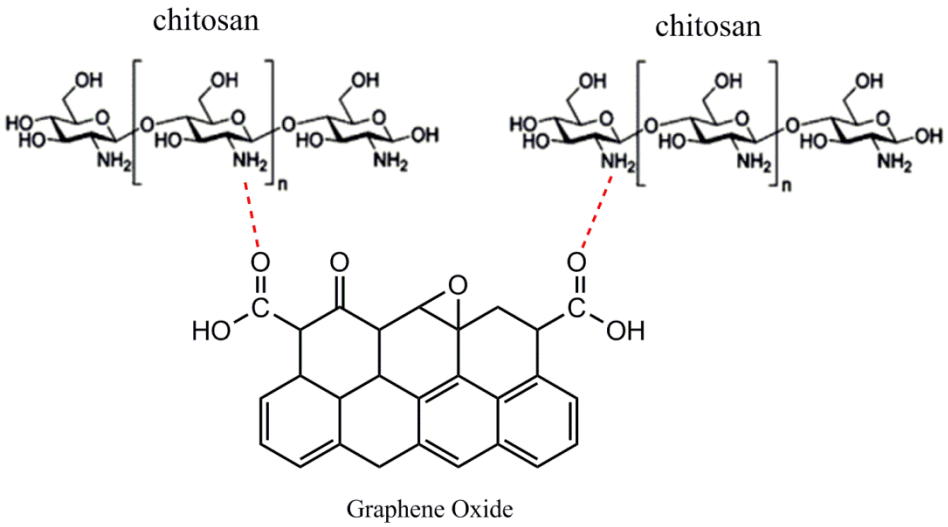

Scheme 2. Chemistry applied for fabrication of GO/CS nanocomposites based glassy carbon electrode.

3. RESULTS AND DISCUSSION

3.1 Characterization of modified electrode

The morphological characterization of graphene oxide was investigated by TEM, as shown in Fig. 1A. The translucent morphology revealed that the graphene had been exfoliated into single-

layered sheets in ultrapure water with ultrasound. It also indicated that GO sheets had a corrugated and layered structure. The SEM image of as-synthesized GO was depicted in Fig. 1B. It can be observed that the two-dimensional structure with several wrinkles and stacking layers [42]. It is clear that the heterogeneous GO/CS nanocomposites distributed uniformly in Fig. 1C [13]. As shown in Fig. 1D, chitosan were inserted into the layer of GO sheet and enlarged its layer distances and width of the wrinkles at higher magnification, which could improve the surface area of electrode.

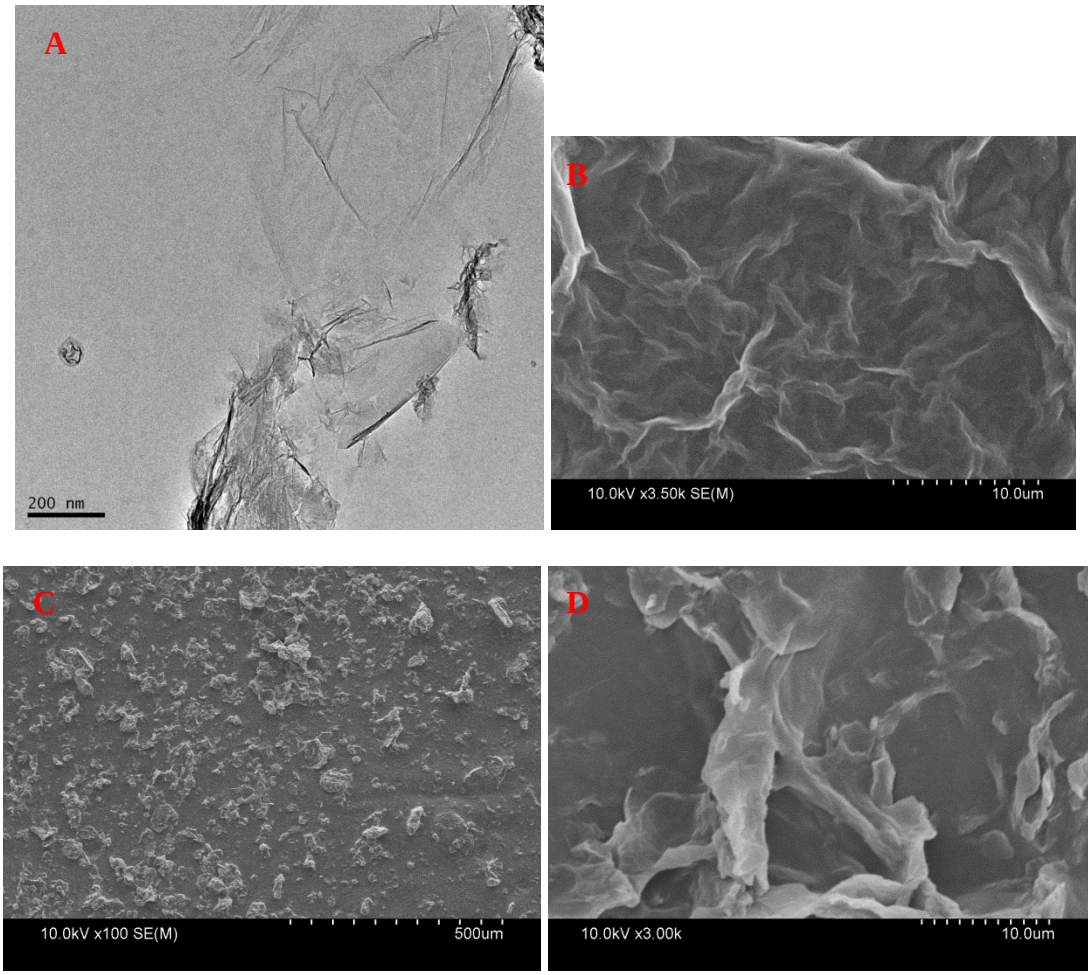

Figure 1. (A) TEM image of the graphene oxide, (B) SEM image of the graphene oxide, (C), (D) SEM images of GO/CS nanocomposites at different magnification.

The FTIR spectra of GO and CS have been shown in Fig. 2. In the spectrum of GO, there was a broad absorption band at 3383 cm^{-1},which are characteristics of $v_{(O-H)}$, and the peaks at 1730, 1612 cm^{-1} are attributed to $v_{(C-O)}$ and $v_{(C=C)}$ of carboxyl group [43]. In the spectrum of CS, the peaks at 1651 and 1593 cm^{-1},which related to the C=O stretching vibration of amide and the N-H bending of amine, respectively [39]. XRD patterns of graphite and GO were shown in Fig. 3, the characteristic 2θ peak of GO appears at 12.36°, and compared with graphite the peak at 26.36° was disappeared. It indicated that graphite transformed into GO completely [44].

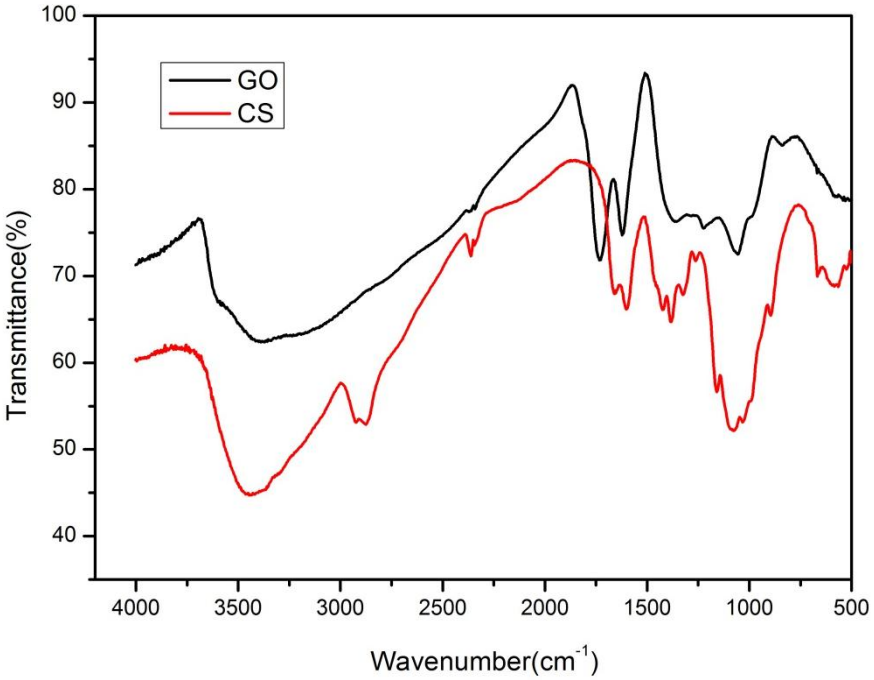

Figure 2. FTIR spectra of graphene oxide and chitosan.

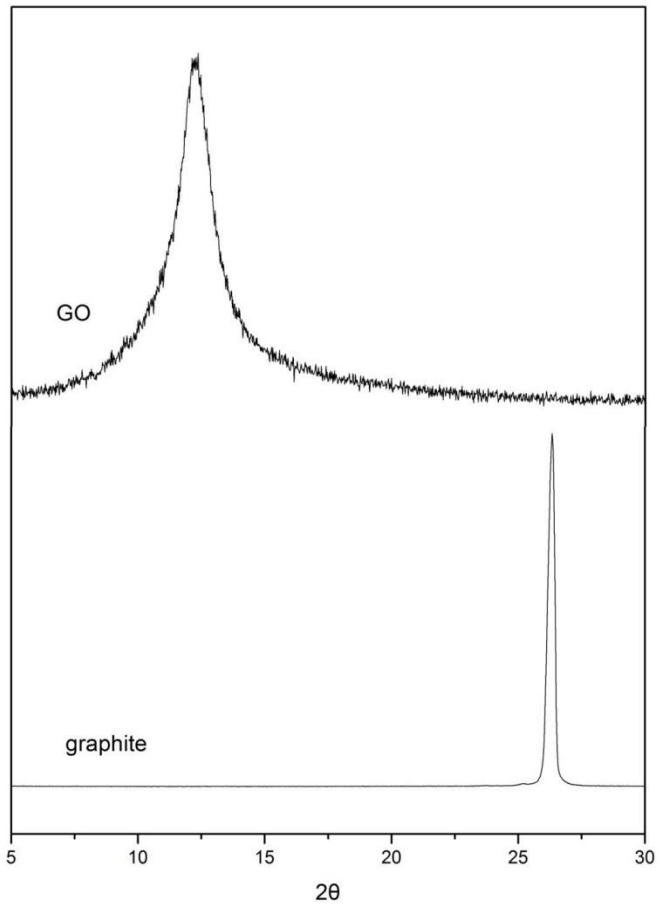

Figure 3. XRD patterns of graphite and GO.

3.2 Electrochemical behaviors of modified electrode

3.2.1 Optimization of the electrode preparation

The proportion of chitosan and graphene oxide affected the electron transfer rate and the amount of DNA loading on the electrode surface [16]. The ratios of GO/CS nanocomposites were expressed as GO/CS-x wt%, where the x is 0.2, 0.4, 0.6 and 0.8. Cyclic voltammetry was used to investigate the electrochemical performance of different mass ratios of GO and CS in nanocomposite (Fig. 4.). From the figure, the current peaks obviously increased with the loading content of 0.4 wt%, which could be corresponded to distributed uniformly GO in CS matrix and better dispersion of GO and the stronger interaction between GO and CS. Therefore, 0.4 wt% was chosen in studies.

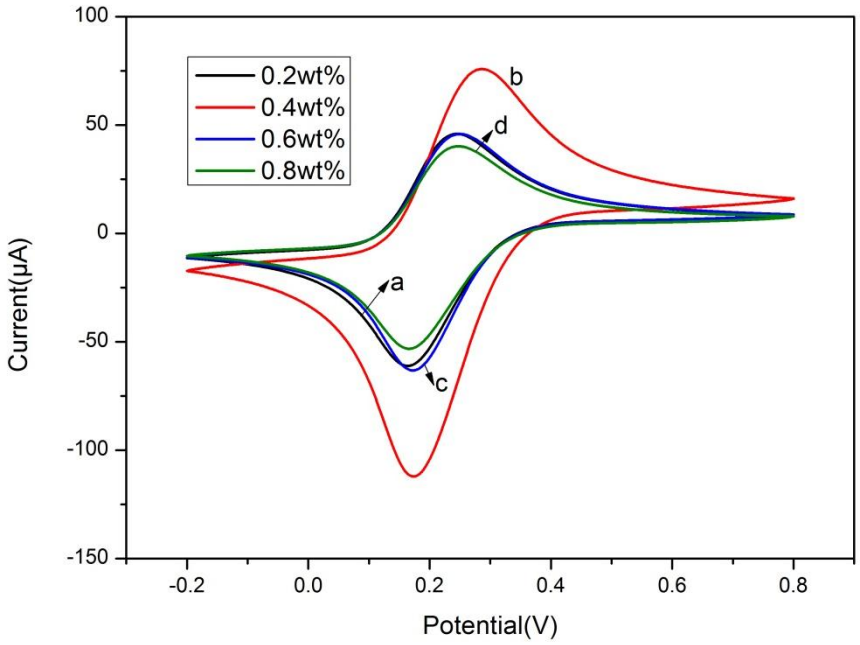

Figure 4. Cyclic voltammograms of GO/CS/GCE electrode at different ratios in 1mM $K_3[Fe(CN)_6]$ solution containing 0.1 M KCl. Scan rate:50 mV/s.

3.2.2 Electrochemical characterization

The electrochemical behaviors of GO/CS/GCE were studied by cyclic voltammetry in 1 mM $K_3[Fe(CN)_6]$ solution containing 0.1 mM KCl at various scan rates (20~160 mV s^{-1}) and is presented in Fig.5A and B. Obviously, the couple of redox peak currents were enhanced with the increase of square root of scan rate (Eqs.(1) and (2)), suggesting that the kinetics of the redox reaction is diffusion controlled [45]. The modified electrode showed a typical quasi-reversible redox reaction with the cathodic and anodic peak current. The large separation of peaks ($\Delta Ep > 0.059$ V) illustrated the quasi-reversible reaction behavior on the electrode surface [46]. The diffusion coefficient "D" of GO/CS/GCE was calculated using Randles–Sevick equation (Eq. (3)).

$$I_{pA}(\mu A) = -19.739\upsilon^{1/2} + 38.03882 \quad R^2=0.99974 \quad (1)$$

$$I_{pc}(\mu A) = 12.81335v^{1/2} - 8.71016 \quad R^2=0.9997 \quad (2)$$

$$I_p = 2.69 \times 10^5 n^{3/2} A D^{1/2} C v^{1/2} \quad (3)$$

Where I_p is the peak current (A), v is scan rate in (V s^{-1}), A is the surface area of the electrode (cm^2), C is the concentration of $K_3Fe(CN)_6$ (here $C=1\times10^{-6}$ mol·cm^{-3}), n is the number of electrons transferred (here n=1). The calculated D was 1.98×10^{-5} cm^2s^{-1}.

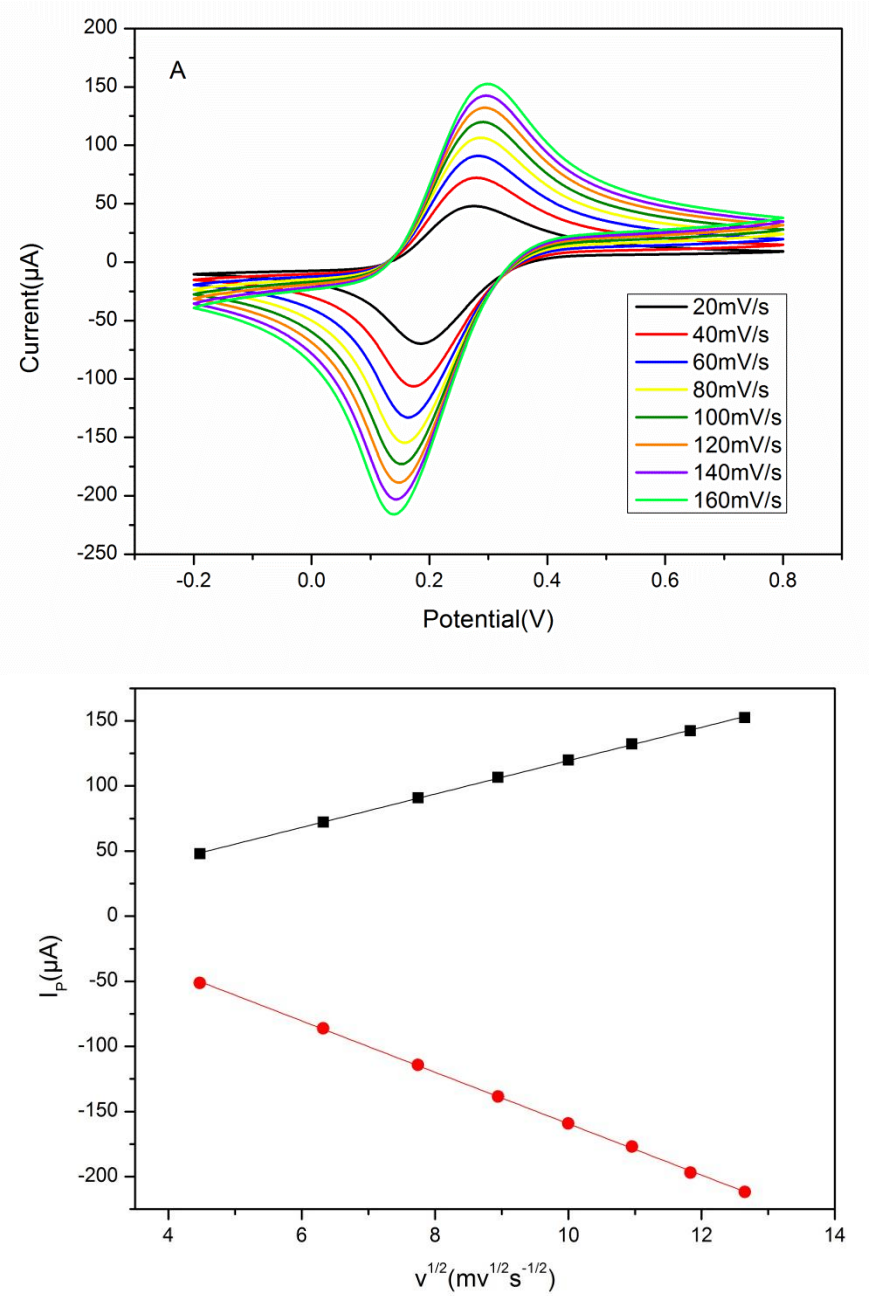

Figure 5. (A) Cyclic voltammograms of GO/CS/GCE at different scan rate in 1 mM $K_3[Fe(CN)_6]$ solution containing 0.1 M KCl. (B) plot of peak currents vs. square root of the scan rate ($v^{1/2}$).

Electrochemical impedance spectroscopy (EIS) is an effective, convenient and label-free method to investigate the interface properties after each assembly step. The semicircle portion observed at higher frequencies of Nyquist plot corresponded to limiting process and a linear part at

lower frequencies represented the the diffusion process. Fig. 6. illustrated the EIS response of bare GCE, CS/GCE, GO/CS/GCE, ssDNA/GO/CS/GCE, dsDNA/GO/CS/GCE. The bare GCE displayed a semicircle with a R_{ct} of about 138 Ω (Fig.6A, curve a). R_{ct} value of CS/GCE reduced to 92.1 Ω (Fig.6A, curve b), this is because CS can be protonated to polycationic material in acid medium. The R_{ct} decreased evidently (Fig.6A, curve c, Fig.6B, curve a, 47.9 Ω), indicating that the addition of GO sheets improve electron transfer kinetics and GO/CS nanocomposite is an excellent electrically conductive material.

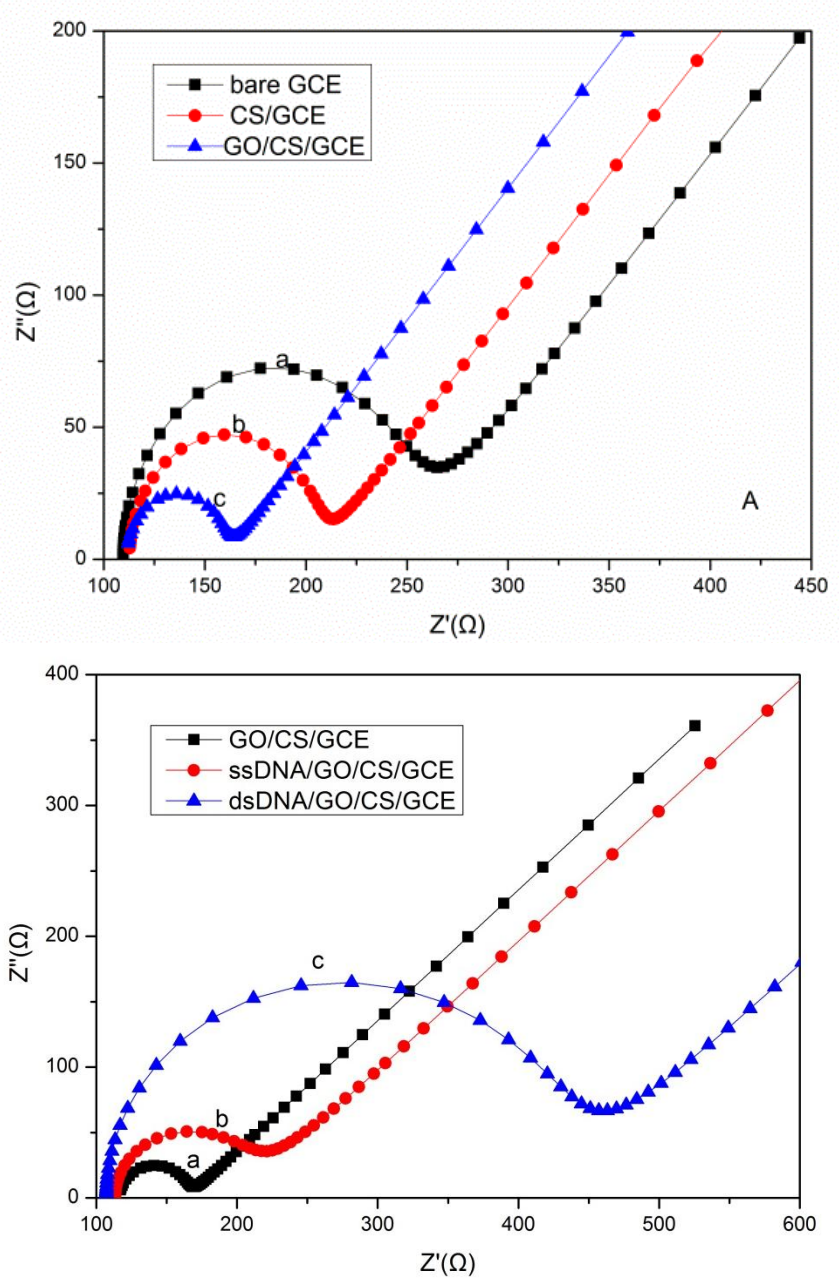

Figure 6. Electrochemical impedance spectroscopy of different modified electrodes in 0.2 mM $[Fe(CN)_6]^{4-/3-}$ solution containing 0.1 M KCl. (A) (a) bare GCE (b) CS/GCE (c) GO/CS/GCE, (B) (a) GO/CS/GCE (b) ssDNA/GO/CS/GCE (c) dsDNA/GO/CS/GCE, the concentration of target DNA was 1×10^{-11} M.

According to Fig.6B, after the ssDNA probe were hybridized with the complementary target sequences, the R_{ct} value of the modified electrode was increased from 92.6 Ω (curve b) to 240.1 Ω (curve c). This results indicated that the repulsion of the negative charge of $[Fe(CN)_6]^{-3/-4}$ and dsDNA at the electrode surface and hindering of the duplex DNA from reaching $[Fe(CN)_6]^{-3/-4}$ the electrode surface [47].

3.3 Optimum conditions for E. coli measurement

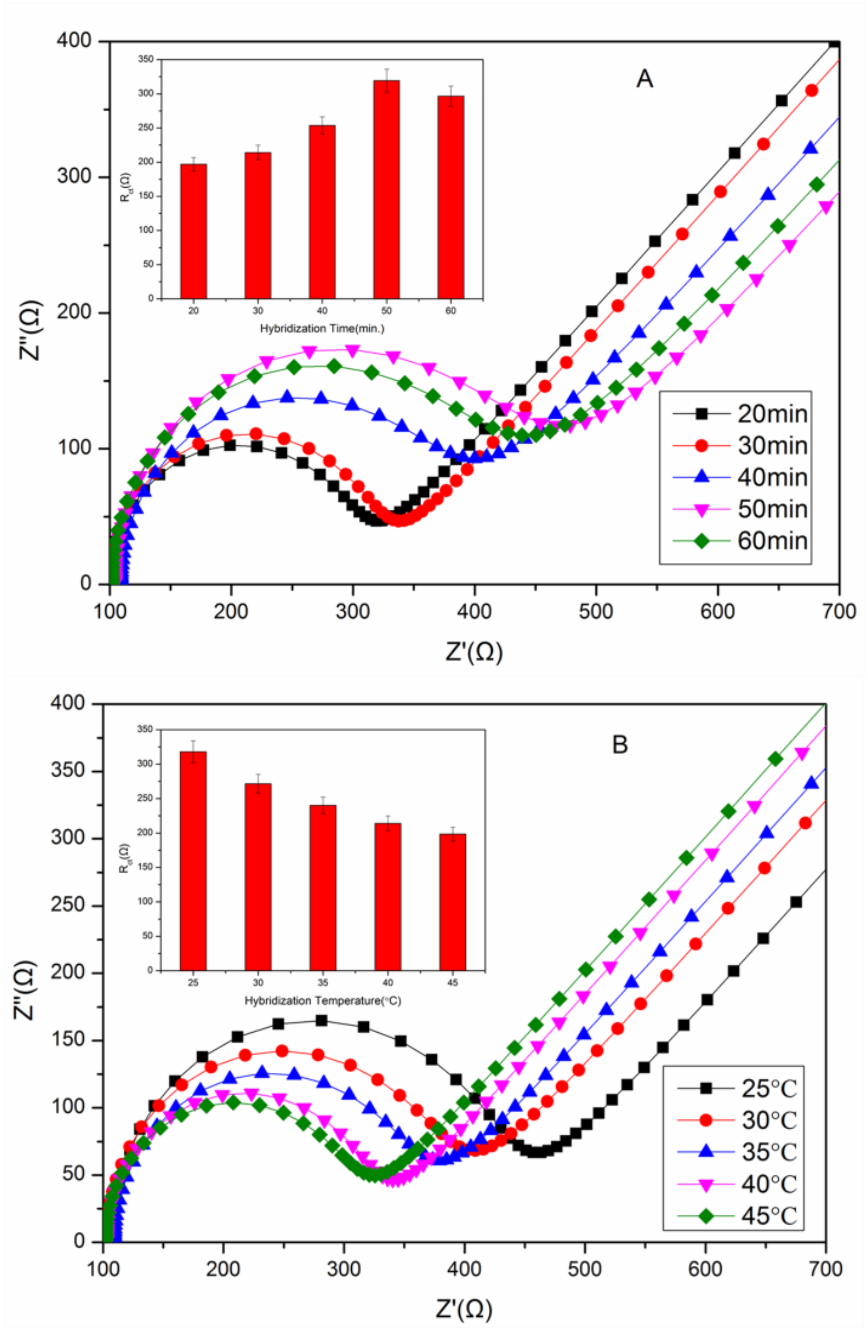

Figure 7. Optimization of operating conditions: (A) effect of time of hybridization for 1.0×10^{-8} M target DNA at 25 ℃. Inset: plot of EIS signals versus hybridization time (B) influence of hybridization temperature for 1.0×10^{-8} M target DNA and hybridization time of 50 min. Inset: polt of EIS signals versus hybridization temperature.

In order to acquire the optimum performance of DNA biosensor, EIS response is a fucntion of investigating the hybridization time and temperature. Fig. 7A displayed the EIS signals after hybridization with 1×10^{-8} M tDNA in incubating time range from 20 to 60 min. It was found that R_{ct} value reached the maximum when duration was 50 min, signifying that it was the optimal time.

DNA hybridization reaction is also closely connected with changing in temperature. Hybridization temperature was variation in range of 25~45 ℃ in the presece of 1×10^{-8} M tDNA. As shown in Fig. 7B, the EIS signals were constant at 25 ℃ and gradually decreased with increasing in temperature. It could be that the temperature is higher than melting temperature thus denaturation of DNA leading to decreasing signals. So, 25 ℃ was currently utilized in experiments.

3.4 Sensitivity of the electrochemical DNA biosensor

The sensitivity of the synthetic DNA biosensor was tested by changing the concentration of complementary target DNA from 1×10^{-14} to 1×10^{-8} M under the optimum conditions (Fig. 7A and B). The different between the R_{ct} value of ssDNA/GO/CS/GCE biosensor and after hybridization with tDNA was used as analytical signal ($\Delta R_{ct}=R_{ct(dsDNA)}-R_{ct(ssDNA)}$). According to Fig. 8, it was found that the EIS signal increased with increasing the concentration. The inset showed the nice relationship between ΔR_{ct} and the logarithm of tDNA concentration. The linear regression equation is $\Delta R_{ct}(\Omega) = 24.65357\log[c(tDNA)] + 417.005$ (R^2=0.9958). The detection limit was calculated to be 3.584×10^{-15} M (3σ,n=5) . It revealed that this method exhibited good sensitivity and lower detection limit compared with previous DNA biosensors (Table 1).

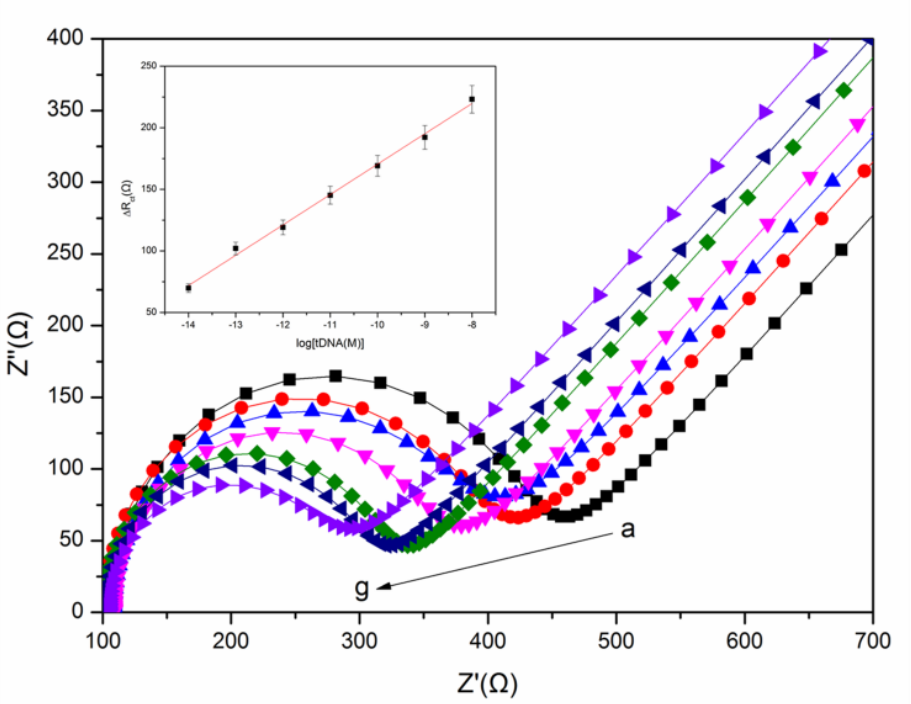

Figure 8. Nyquist plots of ssDNA/GO/CS/GCE biosensor hybridization with different concentrations of complementary DNA (1.0×10^{-14}-1.0×10^{-8} M) in 0.2 mM $[Fe(CN)_6]^{4-/3-}$ solution containing 0.1 M KCl. Inset: plot of ΔR_{ct} versus the logarithm of the target DNA concentrations.

Table 1. Comparison of linear ranges and detection limits of different DNA biosensors.

Modified material of electrode	Detection technique	Linear range	Detection limit	Ref.
CdTe QDs	DPV	1.0×10^{-12}-1.0×10^{-8} M	6.435×10^{-13} M	[48]
SPCE/PLA-AuNPs	DPV	2.0×10^{-13}–2.0×10^{-9} M	5.3×10^{-12} M	[49]
Ga_2Se_3-3MPA	EIS	1.4×10^{-8}-2.0×10^{-8} M	6.6×10^{-10} M	[50]
PAN-nanoZrO_2/PTyr	EIS	1.0×10^{-13}-1.0×10^{-6} M	2.68×10^{-14} M	[51]
GR/TiO_2/CTS	DPV	1.0×10^{-12}-1.0×10^{-6} M	7.21×10^{-13} M	[52]
AuNPs	DPV	2.5×10^{-10}-3.5×10^{-8} M	2.75×10^{-10} M	[53]
GO/CS	EIS	1.0×10^{-14}-1.0×10^{-8} M	3.584×10^{-15} M	This study

3.5 Selectivity of the electrochemical DNA biosensor

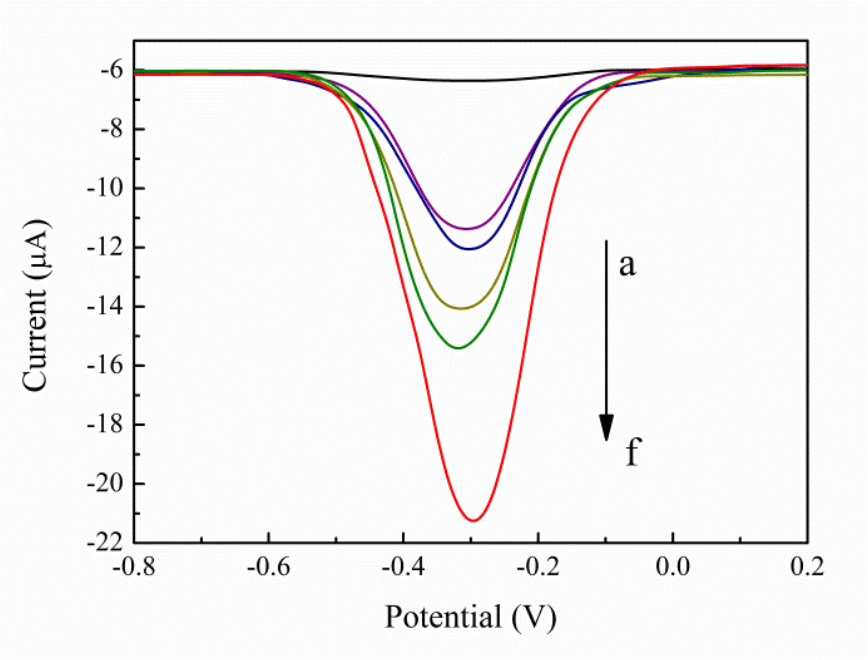

Figure 9. Differential pulse voltammograms of bare GCE (a), MB/ssDNA-probe modified GCE (b), and after hybridized with multi-mismatched ssDNA sequence (c), 2-base mismatched ssDNA sequence (d), 1-base mismatched ssDNA sequence (e), and complementary target ssDNA sequence (f), in the 50 mM Tris-HCl and 20 mM NaCl solution containing 10 μM MB, and concentration of all hybridization DNA sequences was 0.1 μM.

The selectivity of biosensor was investigated by using ssDNA/GO/CS/GCE to hybridize with different ssDNA sequences related to escherichia coli. Fig. 9 showed the DPV responses of MB on the various DNA biosnesors. After hybridization with complementary target ssDNA (curve f), a biggest reduction signal was observed in peak current, indicating that the formation of dsDNA on the surface of GCE had a strong interaction with MB. For one-base mismatched ssDNA sequences (curve e) and two-base mismatched ssDNA sequences (curve d), the DPV signal in paek current was decreased much more than complementary ssDNA sequences, which indicated that only a part of dsDNA had been formed. Simultaneously, after hybridization with multi-mismatched ssDNA sequences (curve c),

the current paek was higher than with MB/ssDNA/GO/CS modified GCE (curve b), and this little increase of peak current was due to the non-specific absorption of ssDNA sequences [54]. These results demonstrated that the modified electrode had satisfactory selectivity in distinguishing different DNA sequences.

3.6 Reproducibility of the electrochemical DNA biosensor

The reproducibility of the electrochemical DNA biosensor was investigated by fabricating five independent electrochemical DNA biosensors under the same conditions. Then these sensors were used to detect 1×10^{-8} M complementary target DNA. The average R_{ct} value of five independent measurements was 318.93 Ω with a relative standard deviation (RSD) of 2.4% for the hybridized electrode. The specific datas shown in Table 2. The results indicated that the electrochemical DNA biosensor was reproducible.

Table 2. Specific data for reproducibility experiments.

n	1	2	3	4	5
R_{ct} (Ω)	318.930	318.947	318.913	318.900	318.959

4. CONCLUSION

In this work, we synthesized a graphene oxide/chitosan nanocomposites modified DNA biosensor for detection of Escherichia coli O157:H7 successfully. The assembly process was investigated with CV and EIS techniques. Due to the addition of GO and CS on the electrode surface, electron transfer rate and biocompatibility were markedly enhanced. Under optimum conditions, the ssDNA/GO/CS/GCE biosensor based on EIS showed a wider detection range (1.0×10^{-14}-1.0×10^{-8} M) and lower detection limit (3.584×10^{-15} M) for target DNA as compared with previously reported biosensors. The fabricated DNA biosensor has been demonstrated to distinguish between complementary DNA, 1-base mismatched DNA, 2-base mismatched DNA and multi-base mismatched DNA by differential pulse voltammetry technique. Therefore, the electrochemical DNA biosensor modified with GO/CS nanocomposites exhibited the superiorities such as easy operation, excellent selectivity, sensitivity and reproducibility, which provided a promising platform to fabricate other electrochemical biosensors.

ACKNOWLEDGEMENTS
This work was supported by the National Natural Science Foundation of China (No. 51678409), andTianjin Science and Technology Development Strategic Plan Project (No.2016KW0001).

References

1. M. H. Abdalhai, A. M. Fernandes, X. Xia, A. Musa, J. Ji and X. Sun, *J. Agr. Food Chem.*, 63 (2015) 5017.

2. S. C. Donhauser, R. Niessner and M. Seidel, *Anal. Chem*., 83 (2011) 3153.
3. R. R. Hu, Z. Z. Yin, Y. B. Zeng, J. Zhang, H. Q. Liu, Y. Shao, S. B. Ren and L. Li, *Biosens. Bioelectron.*, 78 (2016) 31.
4. Y. Li, J. Deng, L. C. Fang, K. K. Yu, H. Huang, L. L. Jiang, W. B. Liang and J. S. Zheng, *Biosens. Bioelectron.*, 63 (2015) 1.
5. S. Y. Wong, A. Paschos, R. S. Gupta and H. E. Schellhorn, *Environ. Sci. Technol*., 48 (2014) 11462.
6. W. Wu, S. Zhao, Y. Mao, Z. Fang, X. Lu and L. Zeng, *Anal. Chim. Acta*, 861 (2015) 62.
7. R. Singh, M. D. Mukherjee, G. Sumana, R. K. Gupta, S. Sood and B. D. Malhotra, *Sens. Actuat. B-Chem.*, 197 (2014) 385.
8. V. Velusamy, K. Arshak, O. Korostynska, K. Oliwa and C. Adley, *Biotechnol. Adv*., 28 (2010) 232.
9. D. L. Zheng, Q. X. Wang, F. Gao, Q. H. Wang, W. W. Qiu and F. Gao, *Biosens. Bioelectron*., 60 (2014) 167.
10. H. P. Peng, Y. Hu, P. Liu, Y. N. Deng, P. Wang, W. Chen, A. L. Liu, Y. Z. Chen and X. H. Lin, *Sens. Actuat. B-Chem*., 207 (2015) 269.
11. F. J. Pavinatto, L. Caseli and O. N. Oliveira, *Biomacromolecules*, 11 (2010) 1897.
12. D. Rao, Q. Sheng and J. Zheng, *Sens. Actuat. B-Chem*., 236 (2016) 192.
13. A. Singh, G. Sinsinbar, M. Choudhary, V. Kumar, R. Pasricha, H.N. Verma, S.P. Singh and K. Arora, *Sens. Actuat. B-Chem*., 185 (2013) 675.
14. L. Q. Luo, L. M. Zhu, Y. H. Xu, L.Y. Shen, X. Wang, Y. P. Ding, Q. X. Li and D. M. Deng, *Microchim. Acta*., 174 (2011) 55.
15. P. J. VandeVord, H. W. T. Matthew, S. P. DeSilva, L. Mayton, B. Wu and P. H. Wooley, *J. Biomed. Mater. Res.*, 59 (2002) 585.
16. L. He, H. Wang, G. Xia, J. Sun and R. Song, *Appl. Surf. Sci*., 314 (2014) 510.
17. B. Balakrishnan, R. Banerjee, *Chem. Rev*., 111 (2011) 4453.
18. S. Emami, H. Ghourchian and A. Divsalar, *Int. J. Biol. Macromol*., 48 (2011) 243.
19. P. Laurienzo, *Mar. Drugs*, 8 (2010) 2435.
20. R. Porta, L. Mariniello, P. Di Pierro, A. Sorrentino and C. V. L. Giosafatto, *Crit. Rev. Food Sci*.,51 (2011) 223.
21. W. S. Wan Ngah, L. C. Teong and M. A. K. M. Hanafiah, *Carbohydr. Polym*., 83 (2011) 1446.
22. H. Yi, L. Q. Wu, W. E. Bentley, R. Ghodssi, G. W. Rubloff, J. N. Culver and G. F. Payne, *Biomacromolecules*, 6 (2005) 2881.
23. Y. Fang, D. Zhang , Y. Guo, Y. Guo and Q. Chen, *Sens. Actuat. B-Chem*., 221 (2015) 265.
24. J. Liu, X. Wang, T. Wang, D. Li, F. Xi, J. Wang and E. Wang, *ACS Appl. Mat. Interfaces*, 6 (2014) 19997.
25. I. Tiwari, M. Singh, C. M. Pandey and G. Sumana, *Sens. Actuat. B-Chem*., 206 (2015) 276.
26. C. Chung, Y. K. Kim, D. Shin, S. R. Ryoo, B. H. Hong and D. H. Min, *Acc. Chem. Res*, 46 (2013) 2211.
27. G. Goncalves, P. A. A. P. Marques, C. M. Granadeiro, H. I. S. Nogueira, M. K. Singh and J. Gracio, *Chem. Mater*., 21 (2009) 4796.
28. W. Li, X. Geng, Y. Guo, J. Rong, Y. Gong, L. Wu, X. Zhang, P. Li, J. Xu, G. Cheng, M. Sun and L. Liu, *ACS Nano*, 5 (2011) 6955.
29. D. Chen, H. Feng and J. Li, *Chem. Rev*. 112 (2012) 6027.
30. Y. Wang, S. J. Zhen, Y. Zhang, Y. F. Li and C.Z. Huang, *J. Phys. Chem*. C, 115 (2011) 12815.
31. Q. Yang, X.J. Pan, F. Huang and K.C. Li, *J Phys. Chem*. C, 114 (2010) 3811.
32. Z. J. Wang, X. Z. Zhou, J. Zhang, F. Boey and H. Zhang, *J. Phys. Chem*. C, 113 (2009) 14071.
33. X. L. Zuo, S. J. He, D. Li, C. Peng, Q. Huang, S. P. Song and C. H. Fan, *Langmuir*, 26 (2010) 1936.
34. Q. Gong, Y. Wang and H. Yang, *Anal. Methods*, 7 (2016) 2554.

35. K. K. Reza, M. A. Ali, S. Srivastava, V. V. Agrawal and A. M. Biradar, *Biosens. Bioelectron*., 74 (2015) 644.
36. Y. X. Fang, E. K. Wang, *Chem. Commun*., 49 (2013) 9526.
37. S. Hajihosseini, N. Nasirizadeh, M. S. Hejazi and P. Yaghmaei, *Mater. Sci. En.g C Mater. Biol. Appl*., 61 (2016) 506.
38. H. Y. Huang, W. Q. Bai, C. X. Dong, R. Guo and Z. H. Liu, *Biosens. Bioelectron*., 68 (2015) 442.
39. X. Yang, Y. Tu, L. Li, S. Shang and X. M. Tao, *ACS Appl. Mater. Interfaces*, 2 (2010) 1707.
40. C. S. Park, H. Yoon and O. S. Kwon, *J. Ind. Eng. Chem*., 38 (2016) 13.
41. W. Suginta, P. Khunkaewla and A. Schulte, *Chem. Rev*., 113 (2013) 5458.
42. Y. Zhang, Z. R. Tang, X. Fu and Y. J. Xu, *ACS Nano*, 4 (2010) 7303.
43. K. B. Ramirez, A. L. M. Hernandez, G. M. Barrera, M. D. Icaza, V. M. Castano and C.V. Santos., *Materials*, 6 (2013) 911.
44. S. Rajabzadeh, G. H. Rounaghi, M. H. Arbab-Zavar and N. Ashraf, *Electrochim. Acta*, 135 (2014), 543.
45. Y. C. Yang, C. Li, L. Yin, M. Y. Liu, Z. X. Wang, Y. Q. Shu and G. X. Li, *ACS Appl. Mater. Interfaces*, 6 (2014) 7579.
46. K. Y. Goud, G. Catanante, A. Hayat, S. M., K. V. Gobi and J. L. Marty, *Sens. Actuat. B-Chem*., 235 (2016) 466.
47. L. Kashefi, M. Mehrgardi, *Biosens. Bioelectron*., 33 (2012) 184.
48. C. Zhang, S. Xu, X. Zhang, D. Huang, R. Li, S. Zhao and B. Wang, *J. Electroanal. Chem*., 735 (2014) 115.
49. N. Nordin, N. A. Yusof, J. Abdullah, S. Radu and R. Hushiarian, *Biosens. Bioelectron*., 86 (2016) 398.
50. 50 P. M. Ndangili, R. A. Olowu, S. N. Mailu, R. F. Ngece, A. Jijana, A. Williams, F. Iftikhar, P. G. L. Baker and E. I. Iwuoha, *Int. J. Electrochem. Sci*., 6 (2011) 1438.
51. J. Yang, X. L. Wang and H. Q. Shi, *Sens. Actuator B-Chem*., 162 (2012) 178.
52. H. Gao, M. Sun, C. Lin and S. Wang, *Electroanalysis*, 24 (2012) 2283.
53. X. Miao, X. Guo, Z. Xiao and L. Ling, *Biosens. Bioelectron*., 59 (2014) 54.
54. W. Sun, Y. Y. Zhang, X. M. Ju, G. J. Li, H. W. Gao and Z. F. Sun, *Anal. Chim. Acta*, 752 (2012) 39.